

# In vivo $^1\text{H}$ MR spectra analysis by means of second derivative method

Maria Sokół \*

*Maria Skłodowska-Curie Institute of Oncology, Department of Medical Physics, Wybrzeże Armii Krajowej 15 Str, 44 100 Gliwice, Poland*

Received 19 June 2000; received in revised form 23 October 2000; accepted 22 November 2000

## Abstract

Short echo time (TE) in vivo PRESS  $^1\text{H}$  MR spectra (2 T, TE = 35 ms) of normal brain were fitted in the frequency domain using the second derivative method. In this approach, local maxima and hidden peaks are found as local minima of spectrum second derivative. The Lorentzian robust minimisation procedure (referred to as maximum likelihood or m-estimate fitting) using Levenburg–Marquardt non-linear fitting engine was applied. Spectral lines were approximated under the assumption of the mixed Lorentzian/Gaussian lineshapes. The same procedure was applied to 18 proton spectra. The number of peaks found within the range of 0.74/4.2 parts per million (ppm) was  $52 \pm 3$  and their positions were almost the same. The fitted lines were assigned on the basis of the J-pattern recalculated for the field strength of 2 T and by comparing the chemical shifts with the shifts in the single compound spectra. The ratios of main metabolites, such as NAA/Cr, Cho/Cr, Cho/NAA and ml/Cr, are in accord with those obtained earlier using the software supplied with the MR imager and the absolute concentrations of *N*-acetylaspartate (NAA), choline containing compounds (Cho), *myo*Inositol (ml), glucose (Glc) and glutamate (Glu) obtained from the fit agree with those reported in literature, which confirms the usefulness of the second derivative method in routine analyses of  $^1\text{H}$  MR brain spectra. © 2001 Elsevier Science B.V. All rights reserved.

*Keywords:* Brain; In vivo  $^1\text{H}$  MRS; Spectra fitting; Second derivative method; Metabolite concentrations

## 1. Introduction

$^1\text{H}$  Magnetic Resonance Spectroscopy ( $^1\text{H}$  MRS) is a non-invasive and non-destructive technique that provides information on metabolism in vivo [1]. There is a growing body of evidence that  $^1\text{H}$  MRS may contribute to the clinical evaluation of a number of pathologies and/or therapeutically induced changes in metabolite concentrations. However, the method suffers from some internal and external limitations that may strongly influence the results. Hardware, software, methodological factors and properties of tissues under study (such as relaxation rates and J-coupling) influence the spectral resolution and, in consequence, the metabolite ratios. The accuracy and precision of spectroscopic quantification is dependent on a hardware performance, the pulse sequence type and its appropriate configuration and localisation [2,3], efficiency of

water suppression and the method used to derive signal intensities from the spectra [4]. The contribution of the latter factor to total error increases with the number of overlapping peaks and degree with which they overlap [5]. Due to a complex J-pattern and line broadening induced by inhomogeneity of the static field in vivo proton spectra constitute extreme case of such a situation [6]. Although spectral assignments usually based on high-resolution spectra of brain tissue or acid extracted brain tissue, however, it is not possible to adopt directly the spectral picture obtained at a spectrometer operating at several hundreds MHz. It should be kept in mind that the chemical shifts of the multiplet components, as measured in parts per million (ppm), depend on the strength of static magnetic field the spectrum is recorded at.

In order to resolve in vivo  $^1\text{H}$  MR spectra fitting algorithms can be applied both in time and frequency domains. On the other hand, resolution enhancement methods may also be used as an alternative for the analysis of raw NMR data [7,8], however, the latter

\* Corresponding author. Tel. +48-322-789363.  
E-mail address: mbsokol@iname.com (M. Sokół).

approach is difficult to be routinely used in clinical practice. In such applications the postprocessing procedure should be fast, simple, reproducible and reliable. However, as reveals from the multicenter studies on the MRS data-analysis [9], fulfilment of the conditions of reliability and reproducibility of proton MRS in brain depends strongly on system and operator variability, as well as on user-interactive steps [10].

The aim of this study was to check the usefulness of the automated fitting method offered by PeakFit 4.0 (by SPSS Inc., Chicago, USA). In this method, local maxima and hidden peaks are found as local minima of the second derivative of the spectrum. The method does not require the starting values (as frequencies and linewidths) to be supplied by the user and is free from the limitations of the fitting software delivered by the manufacturer (such as a limited number of the peaks that can be simultaneously fitted or the lineshape restrictions). It is also worth noting that it is much cheaper since the spectra analyses may be performed on a PC computer.

The accuracy and adequacy of the fitting was checked by a comparison of the relative peak ratios and main metabolites absolute concentrations calculated on the basis of the fitting with the values obtained earlier using the software supplied with the MR imager, as well as with the data reported in literature.

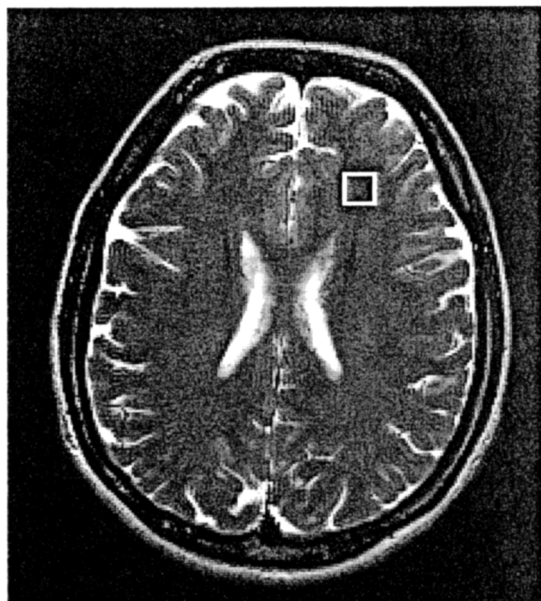


Fig. 1. T2-weighted MR image showing representative VOI ( $1.5 \times 1.5 \times 1.5 \text{ cm}^3 \approx 3.4 \text{ cm}^3$ ) selected for proton MR spectroscopy of white matter in frontal brain.

## 2. Materials and methods

Subjects, who were studied, were 18 healthy volunteers (nine men and nine women) of an average age of  $29 \pm 7$ . They were examined in a whole-body MRI/MRS system (Elscent 2T Prestige) operating at the field strength of 2T and a proton resonance frequency of 81.3 MHz applying the standard head coil. Informed written consent was obtained before all examinations.

MRI localised  $^1\text{H}$  MR spectra were acquired from the volumes of interest of  $1.5 \times 1.5 \times 1.5 \text{ cm}^3$  localised in frontal lobe (white matter) and using a single voxel double-spin-echo PRESS sequence with  $\text{TR} = 1500 \text{ ms}$ ,  $\text{TE} = 35 \text{ ms}$  and 200 Acq. Typical localisation is shown in Fig. 1.

The spectra recording were preceded by the automated global and local shimming procedures. Water suppression was achieved using CHESS technique. Short echo time (TE) of 35 ms was applied since short echo spectra yield more information on brain metabolism and are less suppressed due to relaxation loss of signal intensities. The spectra revealed similar spectral quality, i.e. similar line widths of the water signal (the mean linewidth:  $6.8 \text{ Hz} \pm 0.6$ ) and signal-to-noise ratios.

L-Glutamic acid, D-glucose and *myo*Inositol (mI) (Sigma) aqueous solutions of the concentration of 50 mM were prepared according to [11] and their  $^1\text{H}$  spectra were recorded using the PRESS sequence with the same parameters as in the case of in vivo measurements. The high-resolution  $^1\text{H}$  NMR studies of the solutions in  $\text{D}_2\text{O}$  were performed using a Varian Inova-300 multinuclear pulsed NMR spectrometer operating at the  $^1\text{H}$  resonance frequency of 300 MHz. Chemical shifts in the in vitro proton spectra were measured relative to the solution of sodium 3-trimethylsilylpropionate (TSP) serving as an external standard. Typical  $^1\text{H}$  NMR parameters were, a pulse width of  $31.5^\circ$ , acquisition time of 4.74 s and a spectral width of 4000 Hz.

### 2.1. Spectra processing

Spectra processing involved application of a line broadening of 2 Hz, manual zero- and first-order phase correction, subtraction of the signal due to  $\text{H}_2\text{O}$  and the baseline correction [12, 13]. Finally, the spectra were fitted in the frequency domain using two fitting procedures, the least-squares procedure supplied by the machine manufacturer (program Curvefit by Elscint) and the second derivative method offered by PeakFit (by SPSS Inc., Chicago, USA). The starting parameters for the former were taken from the in vitro spectra of cerebrospinal fluid (CSF) [14], as well as from in vitro NMR studies of rat brains [15,16]. Relative intensities of the signals due to *N*-acetylaspartate (NAA), choline containing compounds (Cho), creatine compounds (Cr)

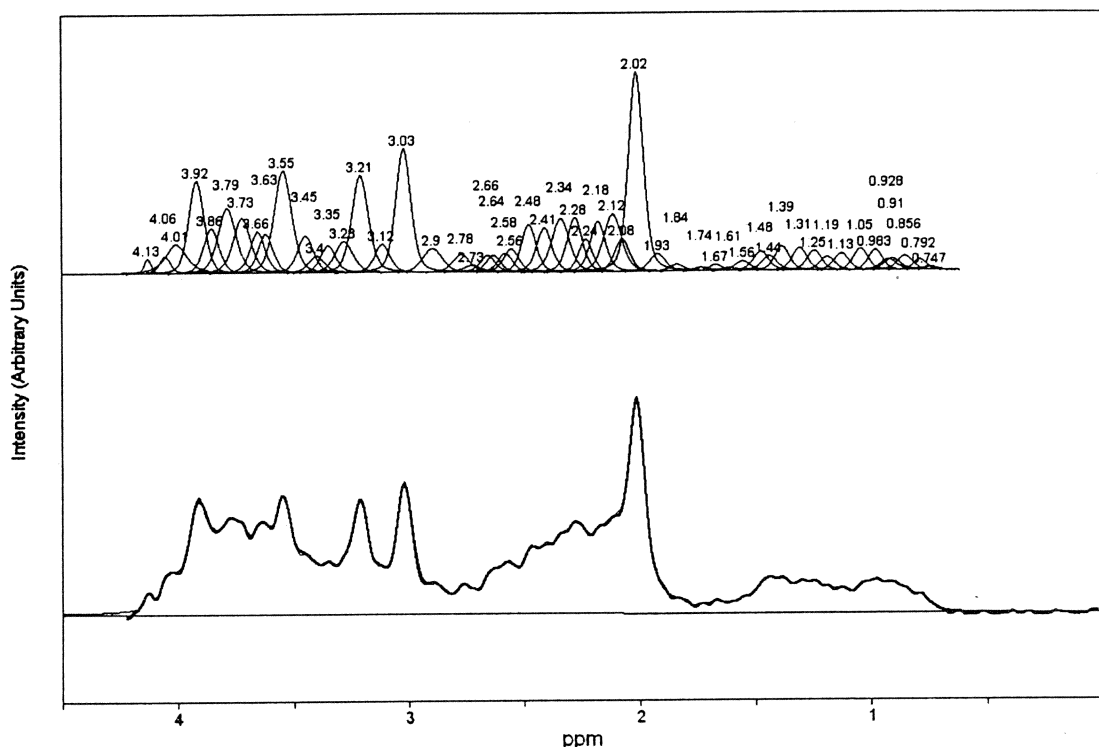


Fig. 2. In vivo  $^1\text{H}$  MR spectrum of human brain obtained at TE = 35 ms and separated automatically into individual components using second derivative method. (a) The fitted components (the chemical shifts shown) (upper graph) and the comparison of the experimental spectrum and that calculated on the basis of fitting (lower graph). Details of fitting: 8192 data points, 214 parameters, fit standard error = 0.10, coefficient of determination  $r^2 = 0.998$ ,  $F = 9368.20$ . (b) The standardised residuals of the fit.

and mI obtained by a numerical integration of the fitted signals of the Lorentzian shape [12] were compared with the corresponding values gained from the method offered by PeakFit. In the latter peaks are detected automatically as second derivative minima. Along with peaks, which are quite apparent in visual inspection hidden ones are also detected. The Savitzky–Golay algorithm was used to produce a smooth second derivative and the smoothing parameter was 1.48%, the value being chosen experimentally to avoid the second derivative peaks (local minima) to be washed out. On the other hand, the rejection threshold was set high enough (2.5%) to discard any sinusoidal effects that appear within or about the baseline, but low enough to include the smallest of the desired peaks.

The Lorentzian robust minimisation procedure (referred to as maximum likelihood or m-estimate fitting) using Levenburg–Marquardt non-linear fitting engine was applied. The fitting was performed up to  $r^2$  value to be at least 0.99. Spectral lines were approximated under the assumption of the mixed Lorentzian/Gaussian lineshapes. Such a lineshape is recommended to avoid an error due to the distortions of the lineshape caused by eddy currents. Moreover, the Lorentzian shape seems to be questionable in case of cluster signals [17]. It should be noted that employing of the mixed

lineshapes is available neither in VARPRO [18] nor in AMARES [19] methods.

### 3. Results

Fig. 2a shows the representative experimental in vivo  $^1\text{H}$  MR spectrum separated automatically into individual components using the second derivative method and the spectrum calculated on the basis of the fitting compared with the experimental one. For the sake of visualisation of the fitting accuracy, the standardised residuals plot is presented in Fig. 2b. The same procedure was applied to all the proton spectra under study. The number of peaks found within the range of 0.74/4.2 ppm was  $52 \pm 3$  and their positions were almost the same. The signals of matching chemical shifts were assumed to correspond to each other whereas those occasionally detected in the spectra were excluded from the analysis as originating from variability within the examined group (metabolic and/or due to spectral resolution). The selection of the signals and signal rejection procedure was automated with a specially prepared program. The line positions varying less than  $\pm 0.02$  ppm were accepted by the program as matching. In case of ambiguous assignment, the normalised areas of

the peaks were compared. Finally, in order to assign the fitted lines their positions were compared with the chemical shifts (in ppm) of the components of metabolite multiplets obtained from the high resolution  $^1\text{H}$  NMR spectra of acid extracts and tissue of rat brain [14,15] recalculated for the field strength of 2 T. In case

Table 1

Centres and areas of peaks located from local minima of second derivative of the  $^1\text{H}$  MR in vivo spectra of the human brain (mean  $\pm$  S.D.,  $n = 18$ )<sup>a</sup>

Main metabolites contributing to individual peaks	Peak centre (ppm)	Peak area
Lac + lip	1.30 $\pm$ 0.01	1.23 $\pm$ 0.44
	1.35 $\pm$ 0.01	1.17 $\pm$ 0.27
Lac	1.39 $\pm$ 0.01	1.10 $\pm$ 0.42
	1.44 $\pm$ 0.01	1.02 $\pm$ 0.40
Ala (?)	1.50 $\pm$ 0.01	1.00 $\pm$ 0.38
	1.56 $\pm$ 0.01	0.93 $\pm$ 0.50
Ala (?)	1.62 $\pm$ 0.01	0.85 $\pm$ 0.41
	1.72 $\pm$ 0.01	0.80 $\pm$ 0.55
	1.78 $\pm$ 0.01	0.70 $\pm$ 0.64
	1.83 $\pm$ 0.01	0.90 $\pm$ 0.55
GABA (?)	1.92 $\pm$ 0.01	1.43 $\pm$ 0.80
GABA	2.02 $\pm$ 0.01	9.15 $\pm$ 1.60
NAA + GABA + Glu	2.09 $\pm$ 0.01	2.62 $\pm$ 0.77
Glu + GABA	2.13 $\pm$ 0.01	2.63 $\pm$ 0.38
Glu	2.19 $\pm$ 0.01	2.45 $\pm$ 0.62
	2.26 $\pm$ 0.02	2.41 $\pm$ 0.58
GABA + Glu	2.31 $\pm$ 0.02	2.52 $\pm$ 0.80
NAA + Glu	2.36 $\pm$ 0.01	2.25 $\pm$ 0.63
GABA	2.41 $\pm$ 0.01	2.17 $\pm$ 0.44
NAA	2.47 $\pm$ 0.01	2.15 $\pm$ 0.48
Asp	2.54 $\pm$ 0.01	1.37 $\pm$ 0.60
NAA	2.58 $\pm$ 0.01	1.37 $\pm$ 0.38
NAA + Asp	2.64 $\pm$ 0.01	1.22 $\pm$ 0.52
NAA + Asp	2.69 $\pm$ 0.01	0.79 $\pm$ 0.34
Asp	2.73 $\pm$ 0.01	0.69 $\pm$ 0.24
NAA	2.79 $\pm$ 0.02	0.73 $\pm$ 0.32
GABA + Asp	2.90 $\pm$ 0.01	1.25 $\pm$ 0.26
Cr + GABA	3.03 $\pm$ 0.01	5.98 $\pm$ 0.76
GABA	3.12 $\pm$ 0.01	1.81 $\pm$ 0.83
Cho + Tau	3.21 $\pm$ 0.01	5.75 $\pm$ 0.92
Tau + sI	3.28 $\pm$ 0.02	1.25 $\pm$ 0.49
Tau	3.35 $\pm$ 0.01	1.39 $\pm$ 0.49
	3.40 $\pm$ 0.01	1.42 $\pm$ 0.52
Glc	3.45 $\pm$ 0.01	1.70 $\pm$ 0.67
mI + Gly	3.55 $\pm$ 0.02	4.04 $\pm$ 0.77
MI	3.63 $\pm$ 0.01	2.17 $\pm$ 0.56
Glu	3.67 $\pm$ 0.01	3.57 $\pm$ 1.44
Glu	3.74 $\pm$ 0.01	3.03 $\pm$ 0.60
Glc + Glu + Ala	3.79 $\pm$ 0.01	2.76 $\pm$ 1.18
Glu + Asp	3.83 $\pm$ 0.01	2.27 $\pm$ 0.60
Asp	3.88 $\pm$ 0.00	2.59 $\pm$ 0.88
Cr + Asp	3.93 $\pm$ 0.01	4.59 $\pm$ 1.38
Lac	3.97 $\pm$ 0.01	1.48 $\pm$ 0.58
MI	4.02 $\pm$ 0.01	1.23 $\pm$ 0.45
mI + Lac	4.06 $\pm$ 0.01	1.22 $\pm$ 0.60

<sup>a</sup> Abbreviations: Ala, alanine; Asp, aspartate; GABA, g-aminobutyric acid; Cho, choline containing compounds; Glc, glucose; Glu, glutamate; Gly, glycine; Lac, lactate; mI, myoinositol; NAA, N-acetylaspartate; Cr, creatine and phosphocreatine; Tau, taurine.

of multiplets of complex structure, as for glucose, glutamate or mI, the centres of the bands were obtained from the spectra of aqueous solutions of appropriate metabolite. The lines found as common in the analysed spectra are listed in Table 1. Their chemical shifts and normalised areas are averages of 18 measurements.

It should be noted, however, that the overall number of metabolites that are expected to contribute to a  $^1\text{H}$  MR brain spectrum is much larger. For instance the resonances originating from macromolecules, such as cytosolic proteins, lipids and other membrane-bound and/or partially immobilised compounds may overlap signals of low molecular weight metabolites causing the integral intensities of the latter to be overestimated. The overestimation is especially of importance in the most crowded region between 1.9 and 4.5 ppm. Thus, the accurate assignment of the lines found by the automated fitting procedure requires the information on the contributions of other spectral components into the analysed signal, similarly as in case of the fitting methods using prior knowledge.

#### 4. Discussion

The metabolite proportions were calculated using normalised areas of the fitted lines corresponding to the appropriate metabolites and compared with the values obtained earlier with the fitting program supplied with the MR imager [12] (Table 2).

The absolute concentrations of metabolites were determined with the formula [20]

$$[c_i] = \left( \frac{I_i}{I_{Cr}} \right) \left( \frac{f_{Cr}}{f_i} \right) \left( \frac{N_{Cr}}{N_i} \right) [c_{Cr}] \quad (1)$$

where  $c$  is the concentration,  $I$  denotes the integral intensity of the appropriate resonance,  $f$  is the correction factor for the relaxation effects due to  $T_1$  saturation and  $T_2$  dephasing and  $N$  is a number of protons contributing to a given signal. Creatine was assumed to be an internal standard of a concentration of 5.7 mM (the value reported as a creatine concentration in white matter of a frontal lobe) [21]. Although creatine is frequently used as a reference due to a stability of its concentration within each tissue type, it should be, however, noted that the total Cr concentration in human brain in vivo exhibits a heterogeneous regional distribution, which makes the comparison of the results difficult. As reported, the total Cr concentration increases significantly from cortical white matter (5.5–5.7 mM) to gray matter (6.4–7.0 mM) and cerebellum (8.7–9.0 mM) [21]. In consequence, using Cr as an internal standard may result in an additional source of variability for mixed gray and white matter volumes.

The correction factor  $f$  in the Eq. (1) is described as follows [1,22]

Table 2

Comparison on metabolite proportions (mean  $\pm$  S.D.) obtained from in vivo  $^1\text{H}$  MR spectra of human brain (frontal lobe white matter) analysed with the least-squares ( $n = 30$ ) and second derivative methods ( $n = 18$ )

Fitting method	NAA/tCr	Cho/tCr	Cho/NAA	mI/Cr	Glc/Cr	Glu/Cr
Least-squares	1.55 $\pm$ 0.18	0.94 $\pm$ 0.13	0.65 $\pm$ 0.17	0.73 $\pm$ 0.15	— <sup>a</sup>	— <sup>a</sup>
Second derivative	1.53 $\pm$ 0.23	0.98 $\pm$ 0.20	0.64 $\pm$ 0.13	0.69 $\pm$ 0.17	0.30 $\pm$ 0.14	2.10 $\pm$ 0.41
<i>P</i> values <sup>b</sup>	0.78	0.48	0.84	0.46		

<sup>a</sup> Not determined.

<sup>b</sup> *P* values calculated for comparisons between results yielded by both methods.

$$f = \left( 1 - \exp\left(\frac{-\text{TR}}{T_1}\right) \right) \exp\left(\frac{-\text{TE}}{T_2}\right) \quad (2)$$

where TR is a repetition time, TE is an echo time and  $T_1$  and  $T_2$  are spin–lattice and spin–spin relaxation times. The correction factors were calculated using the metabolite relaxation  $T_1$  times (obtained at 2 T) of 1408 ms for NAA, 1438 ms for Cho, 1726 ms for mI, 1554 ms for Cr [23, 24], whereas for glucose (Glc) and glutamate (Glu) the upper value of the  $T_1$  range was applied [22]. The correction of resonance areas for  $T_2$  attenuation was based on relaxation times (at 2 T) of 370 ms for NAA, 360 ms for Cho, 220 ms for Cr, 130 ms for mI and 130 ms for Glu and Glc (strongly coupled) [22]. The corrected values are presented in Table 3. Unfortunately, due to limited number of works concerning the relaxation measurements, the relaxation times used in this study derive from different references, which may affect the concentration values. On the other hand, as reveals from the comparison of the  $T_1$  and  $T_2$  relaxation times reported in different studies for different brain regions there is a general agreement between the findings [22,23,24].

Comparison of the main metabolite ratios obtained with both the methods shows a close agreement, which is confirmed by the statistical analysis of the results with two-sided unpaired *t*-test. The high *P*-values yielded by the test seem to prove low significance of the results difference (Table 2). Automated fitting of the spectra with the second derivative method enables, however, other metabolite ratios, as for example that of Glc to Cr and Glu to Cr (Table 2), as well as the absolute concentrations of these metabolites (Table 3) to be also estimated.

Table 3

Absolute concentrations (mean  $\pm$  S.D.,  $n = 18$ ) of major metabolites in vivo (in mM) calculated on the basis of the second derivative analysis of the  $^1\text{H}$  MRS spectra of human brain<sup>a</sup>

NAA (mM)	Cr (mM)	Cho (mM)	mI (mM)	Glc (mM)	Glu (mM)
7.8 $\pm$ 1.2	5.7	1.7 $\pm$ 0.3	5.0 $\pm$ 1.1 <sup>b</sup>	1.4 $\pm$ 0.5 <sup>c</sup> 1.1 $\pm$ 0.4 <sup>d</sup>	10.5 $\pm$ 3.1 <sup>e,f</sup>

<sup>a</sup> The values of the concentrations were corrected taking into account relaxation effects due to  $T_1$  saturation and  $T_2$  dephasing.

<sup>b</sup> The concentration was calculated from the total area of the lines at 3.55 and 3.63 (assigned to four *myo*inositol protons).

<sup>c</sup> The concentration was calculated from the area of the glucose signal at 3.44 ppm (assigned to four glucose protons).

<sup>d</sup> The area the glucose signal at 3.44 ppm was assigned to a sum of four glucose protons and one of taurine.

<sup>e</sup> The concentration was calculated from the total area of the peaks located at 2.09, 2.13, 2.19, 2.31, 2.36 ppm and assigned to four protons.

<sup>f</sup> The value is overestimated due to an overlap of the Glu signals by those of NAA, GABA and glutamine.

The average value of the Glc/Cr ratio (0.3  $\pm$  0.14) was obtained from the area of the Glc peak centred at 3.44 ppm (Fig. 2a). As seen from the comparison of the 81.3 and 300 MHz proton spectra of the aqueous solutions of glucose (Fig. 3), the line at 3.44 ppm is in fact a multiplet. Since the resonances between 3.1 and 4.1 ppm correspond to 12 glucose protons and the contribution of the line at 3.44 ppm to the total area of that part of glucose spectrum equals ca. 30%, the line at 3.44 ppm may be considered as representing four protons (Fig. 3). Thus, assuming the contribution from SCH<sub>2</sub> group of taurine (Tau) into its total integral intensity to be negligible [22] the absolute concentration of cerebral glucose calculated from the fit and corrected for the relaxation effects would be of ca. 1.4  $\pm$  0.5 mM. In opposite case, assuming the central triplet line of SCH<sub>2</sub> group to incorporate into the line at 3.44 ppm, the latter would be due to five protons and 4/5 of its area would derive from glucose. When taking into account that the concentration of Tau is similar to that of Glc (ca. 1 mM) it leads to a glucose concentration of 1.1  $\pm$  0.4 mM. Michaelis et al. [22] reported the values of 1.0  $\pm$  0.2 mM (white matter) and 1.1  $\pm$  0.2 mM (gray matter), Gruetter et al. [25] obtained the value of 1.0  $\pm$  0.1 mM (as measured by  $^{13}\text{C}$  NMR), whereas Pouwels et al. [21] estimated glucose concentration using the LCModel to be of about 0.6  $\pm$  0.4 mM. On the other hand, Pfeuffer et al. [11] measured the glucose level in rat brain and obtained the value of 2.7  $\pm$  0.2 mM (in vivo  $^1\text{H}$  MRS at 9.7 T). The high value of a standard deviation (S.D.) in this study ( $\pm$  0.4) seems to reflect rather the interindividual variability of the cere-

bral glucose levels in the brain tissue of the studied subjects (the plasma glucose levels were not assigned and presumably differed) than the inaccuracy of the MRS quantification method. As it has been recently demonstrated, the brain glucose level is a linear function of plasma glucose concentration [26]. In experiments where steady-state plasma glucose content was varied from euglycemic to 30 mM, at the upper plasma glucose concentration level the value of the brain glucose concentration approached 9 mM. On the other hand, the decrease was also reported (to 0.8 mM) during photic stimulation [27].

The Glu/Cr ratio value was calculated from the total area of the peaks at 2.09, 2.13, 2.19, 2.31, 2.36 ppm detected in the Glu aqueous solution  $^1\text{H}$  MR spectrum recorded at 2 T as distinct signals. The Glu/Cr ratio obtained in such an approach is  $2.10 \pm 0.41$  and the *in vivo* absolute Glu concentration corrected for the  $T_1$  and  $T_2$  relaxation effects equals  $10.5 \pm 3.1$  mM. This value falls within the range of those reported for white ( $8.1 \pm 1.5$  mM) and gray matter ( $12.5 \pm 3.0$  mM) [20], however is higher than the value of  $7.0 \pm 2.6$  mM reported for white matter of frontal lobe [21]. Due to a spectral superposition of the Glu lines at 2.09, 2.31 and 2.36 ppm with those of NAA and GABA (Table 1), the calculated value of the Glu concentration seems thus to

be overestimated. Another source of the overestimation may be due to neglecting a contribution of the glutamine methylene resonances into the Glu signals. Although Michaelis et al. [22, 28] claim that such a contribution is not expected to be of importance for the healthy brain tissue, Pouwels et al. [21] calculated it to be of ca. 20%.

The concentrations of *N*-acetylaspartate and choline obtained from the fitting and corrected for the relaxation effects ( $7.8 \pm 1.2$  and  $1.7 \pm 0.3$ , respectively) (Table 3) correlate well with the range of published data. Michaelis et al. [22] report the concentrations of  $7.8 \pm 1.0$  (NAA) ( $P = 1$ ) and  $1.6 \pm 0.3$  (Cho) ( $P = 0.24$ ) whereas Pouwels et al. [21] provide the values of  $8.1 \pm 0.9$  ( $P = 0.37$ ) and  $1.78 \pm 0.9$  ( $P = 0.4$ ). The NAA concentration calculated from the singlet at 2.02 ppm agrees also with the biochemical data (4.5–9.5 mM [29]), however, that estimated from the area of the doublet of doublets centred at 2.7 ppm is higher and equals  $9.6 \pm 2.7$  mM. The increased value may result from a superposition of two peaks of the NAA multiplet (at 2.64 and 2.69 ppm) with the corresponding components of the aspartate multiplet. It should be noted that NAAG (*N*-acetylaspartylglutamate) was not recognised in the spectra. Its singlet line of  $\text{CH}_3$  group is expected at 2.05 ppm [11], however no signal was

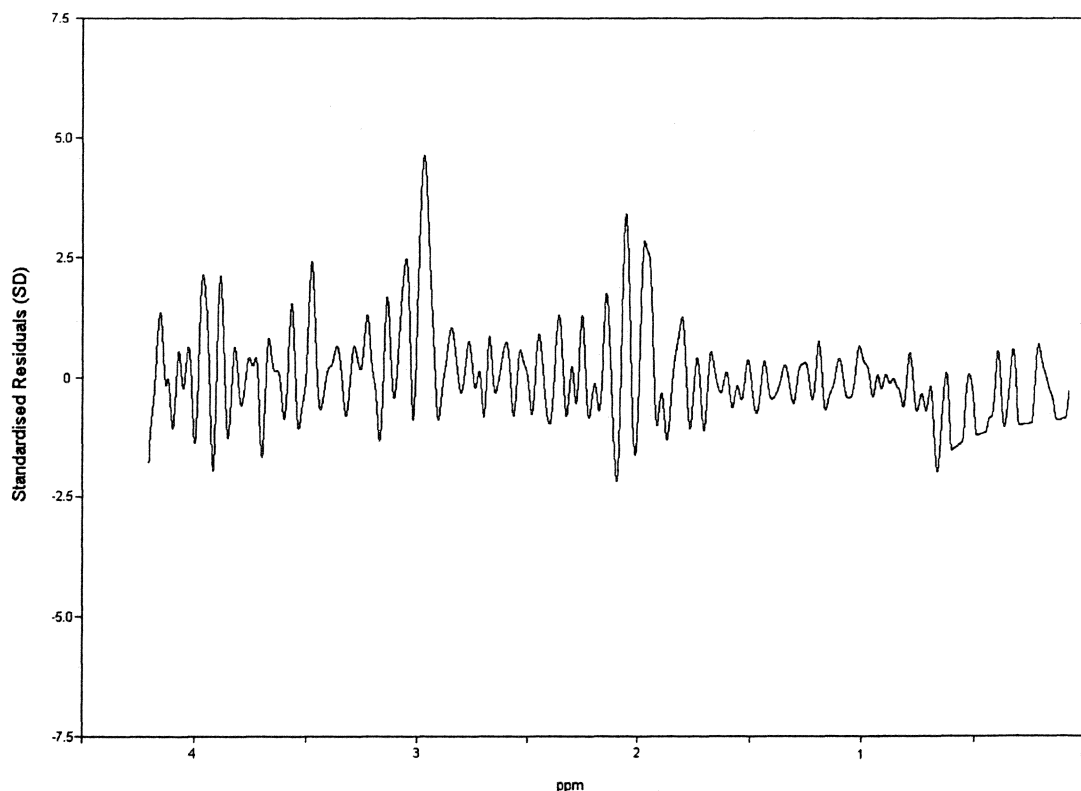


Fig. 3. Comparison of the 81.3 and 300 MHz  $^1\text{H}$  MR spectra of the aqueous solutions of glucose (the spectral range of 3.1–4.2 ppm shown). As revealed from the fitting the overlapped multiplet at 3.44 ppm encompasses about 30% of this part of the spectrum.

found by the second derivative method in the spectral region of  $2.05 \pm 0.02$  ppm (Table 1). Since the NAAG concentration in frontal white matter is only about 18% of that of NAA [21], the  $T_1$  saturation and  $T_2$  relaxation effects may be responsible for the absence of the signal. The distribution of the residuals seems to confirm the supposition. Almost all studied spectra show the highest residual values ( $> 3$  S.D.) at 2.05 and 2.97 ppm (Fig. 2b). The former value may thus reflect the error due to NAAG omitting.

The mI concentration values calculated from the fit and corrected for the  $T_1$  saturation and  $T_2$  relaxation effects ( $5.0 \pm 1.1$  mM) and those reported by Michaelis et al. [22] for white matter ( $3.9 \pm 0.9$  mM) and by Pouwels et al. [21] for white matter of frontal lobe ( $3.8 \pm 0.9$  mM) differ statistically ( $P < 0.01$ ), however in a  $^{13}\text{C}$  NMR studies concentrations of 4.7–7.2 mM were found with use of an absolute reference method [30].

In conclusion, the automated fitting enables reasonable metabolite ratios and absolute concentrations to be obtained, however it should be kept in mind that the second derivative follows only the shape of the curve that represents the sum of all metabolites. Some additional studies are required in order to check the precision of assignments.

#### Acknowledgements

This work was supported by the KBN grant No. 4 PO5B 007 17. The author also wishes to thank Professor Jerzy Walecki and Dr Piotr Pieniążek for their support as well as to Dr Waldemar Przybyszewski for preparing the samples for the NMR studies.

#### References

- [1] Salibi N, Brown M. Clinical MR Spectroscopy. First Principles. New York: Wiley, 1998.
- [2] Bovee WMMJ, Keevil SF, Leach MO, Podo F. Quality assessment in in vivo NMR spectroscopy in medicine. *Magn Reson Imag* 1995;13:123–9.
- [3] Keevil SF, Barbiroli B, Leach MO, Longo R, Lowry M, Moore C, Moser E, Segebarth C, Bovee WMMJ, Podo F. Quality assessment in in vivo NMR Spectroscopy: IV. A multicenter trial of test objects and protocols for performance assessment in clinical NMR spectroscopy. *Magn Reson Imag* 1995;13:139–57.
- [4] Keevil SF, Barbiroli B, et al. Absolute metabolite quantification by in vivo NMR spectroscopy: II. A multicenter trial of protocols for in vivo localised proton studies of human brain. *Magn Reson Imag* 1998;16(9):1093–106.
- [5] van den Boogaart A, ala-Korpela M, Jokisaari J, Griffiths JR. Time and frequency domain analysis of NMR data compared: an application to 1D 1H spectra of lipoproteins. *Magn Reson Med* 1994;31:347–58.
- [6] De Graaf AA, Bovee WMMJ. Improved quantification of in vivo 1H NMR spectra by optimisation of signal acquisition and processing and by incorporation of prior knowledge into spectral fitting. *Magn Reson Med* 1990;15:305–19.
- [7] Cambell ID, Dobson CD, Williams RJ, Xavier A. Resolution enhancement of PMR spectra using difference between a broadened and normal spectrum. *J Magn Reson* 1973;11:172–81.
- [8] Kupka T, Pasterna G, Wojtek P, Nożyński J. Wpływ cyfrowej obróbki widm NMR na dokładność wyznaczania względnej zawartości wybranych metabolitów oraz pH w tkankach. *Rez Magn Med* 1997;5(2):10–5.
- [9] De Beer R, Barbiroli B, Gobbi G, Knijn A, Kugel H, Langenberger KW, Tkac I, Topp S. Absolute metabolite quantification by in vivo NMR spectroscopy: III. Multicentre 1H MRS of the human brain addressed by one and the same data-analysis protocol. *Magn Reson Imag* 1998;16(9):1107–11.
- [10] Webb PG, Sailasuta N, Kohler SJ, Raidy T, Moats RA, Hurd RE. Automated single-voxel proton MRS: technical development and multisite verification. *Magn Reson Med* 1994;31:365–73.